The 15th International Symposium on Magnetic Bearings, August 3-6, 2016, Mojiko Hotel, Kitakyushu, Japan

ISMB15

Inertial Centering of Magnetically Suspended Flexible Rotors

Rami LEVY* and Shai AROGETI*

* Dept. of mechanical Engineering, Ben-Gurion University of the Negev

P.O.B. 653, Beer-Sheva, 8410501, Israel

E-mail: levyram@post.bgu.ac.il, arogeti@bgu.ac.il

Abstract

When an unbalanced flexible rotor reaches a steady state, where it is not vibrating but spinning with a constant geometric shape, it can be assumed (to some extent) a rigid body. Under this assumption, an inertial centering controller is developed for a general flexible AMB-rotor system with multiple mass imbalances. It is shown that in the absence of gyroscopic effects, the inertial center of a discretized flexible rotor can be observed as an independent set of coordinates with static and dynamic imbalance. However, more information is needed to implement an imbalance compensation in the presence of gyroscopic effects. In addition, the stability of the closed loop system is discussed and a case study of 8-DoF flexible rotor is presented. The theory is approved by numerical simulations which result in a complete suppression of more than 420N synchronous force.

Key words : Inertial centering, Flexible rotor systems, Rotor dynamics, Magnetic bearings

1. Introduction

Many high speed rotating systems are supported by Active Magnetic Bearings (AMBs) which allow contact-less operation. Compared to other bearing types, the main advantages of AMBs are due to, their operation with no friction, the little required maintenance compared to standard bearings, and their suitability to vacuum conditions. In addition, the air gap between static and dynamic parts in the AMB can be actively controlled, which allows the rotor to whirl without physical constraint. This feature is important for applications that require minimum vibrations and minimum forces acting on the rotor supports (and hence, minimum control efforts applied by the AMBs). To achieve these operation conditions, the rotor has to be spinning in the direction of its inertial center and hence this approach is referred to as *inertial centering*. On the contrary, in the *geometric centering* control approach, the goal is to achieve a precise position of the rotor axis, that is typically coincides with the geometric center of the bearings. In either cases, mass imbalance plays an important role as a source of disturbance, and this problem is conventionally solved by offline mechanical balancing.

Using the active nature of AMBs, it is possible to implement imbalance compensation for inertial or geometric centering, in real time. Examples have been presented by Lum et al. (1996) and Lum et al. (1998), where inertial and geometric centering were implemented (respectively). These approached included an adaptive imbalance compensation framework that is based on direct estimation of mass imbalance coefficients. A geometric centering control, with an integrated least mean square algorithm for imbalance compensation is given by Xiang and Wei (2014). An inertial centering control with a generalized notch filter for imbalance compensation and an adaptively tuning loop for control currents adjustment is given by Zheng and Feng (2015). These examples, are all for rigid rotors and are implemented in a decentralized scheme. Hence, they do not properly consider the dynamic mass imbalance, which excites gyroscopic moments.

The gyroscopic coupling problem can be solved indirectly by means of advanced robust control methods such as H_∞ and H_2, see for example Fang et al. (2013). The challenge with these methods is to find the required accurate AMB-rotor system model and to formulate the uncertainty and disturbance such that the least conservative controller is achieved. Advanced robust control theory is also the main approach used for flexible rotor systems, which are in general more complex due to their higher dimensionality (e.g., Becker et al (2015), Schittenhelmet et al (2015), Tang et al (2015a), Riemann et al (2013), Sahinkaya et al (2011)). Some works have utilized simplified models to describe the flexible rotor dynamics; models that may facilitate the controller design process. For example, Yuan et al (2013) have modeled the flexible rotor as a rigid shaft and a rigid disk that are interconnected by couples of springs and dampers. Tang et al (2015b) have formulated a simplified model for control, at specific bending critical speeds by modal separation techniques.

In general, the rotor is considered inertially centered if it is spinning in the direction of its principal axis of inertia and through its center of mass. It is clear that, if a rigid rotor is inertially centered, it applies zero radial forces and zero gyroscopic moments on its supports. As to a flexible rotor, some conditions have to be met, before it reaches a steady state where it is spinning with a consistent geometric shape (i.e. a bent rotor) and can be regarded as rigid. This concept was first suggested by Levy and Arogeti (2014), where an inertial centering approach for flexible rotor systems was introduced and a controller was developed for an eight degrees of freedom (DoFs) flexible rotor system, subjected to a single mass imbalance. Here, the method is extended to a general rotor model with multiple mass imbalances and the stability of the closed loop system is further discussed.

2. Methodology

When a flexible rotor is spinning with a constant geometric shape, it can be regarded as a rigid rotor. Indeed, if a radially symmetric flexible rotor system is subjected to a synchronous excitation, then the orbit of the rotor center-line at each cross-section is circular with a frequency ω, that is equal to the frequency of the spin-speed, Ω (i.e. synchronous circular whirl). Hence, the mass elements of the rotor do not carry relative motion since they all orbit in a circular motion of constant radius and frequency. Then, the mass center and the principal axis of the flexible rotor can be calculated based on a rigid body analysis.

2.1. Inertial Center of a Flexible Rotor

The inertial center of a bent rotor is developed based on a lumped mass approach, where a finite set of rigid bodies, i.e., rigid rotors, are lumped by massless elastic fields. The rigid rotors are assumed to be radially symmetric disks or cylinders. Each rotor mass, m_i, is free to translate and rotate in two mutually perpendicular directions and hence the DoFs of each mass element are $x_i, y_i, \theta_{xi}, \theta_{yi}$. The location of each mass along the axial direction is given by z_i. Followed by the assumption that the translations and rotations are sufficiently small, the inertial center of the complete rotor system is defined as the coordinates of the center of mass and principal angles, as follows (Levy and Arogeti, 2014),

$$\begin{array}{lll} M_{tot}x_c = \Sigma_i\left(m_i x_i\right) & , & I_{tot}\theta_{xc} = \Sigma_i\left(\left(I_{ti}-I_{pi}\right)\theta_{xi} - m_i y_i z_i\right) \\ M_{tot}y_c = \Sigma_i\left(m_i y_i\right) & , & I_{tot}\theta_{yc} = \Sigma_i\left(\left(I_{ti}-I_{pi}\right)\theta_{yi} + m_i x_i z_{ii}\right) \end{array} \tag{1}$$

where I_{pi}, I_{ti} are polar and transverse moments of inertia and M_{tot},I_{tot} are the total mass and transverse moment of inertia of the complete rotor, given by $\Sigma_i m_i$ and $\Sigma_i\left(I_{ti}+m_i z_i^2\right)$ respectively.

It is assumed here that each rigid rotor carries a static imbalance, expressed by mass center deflection and dynamic imbalance, expressed by inertial axis inclination. In the following, upper-case letters indicate geometric center coordinates and angles $(X, Y, \Theta_x, \Theta_y)$ and lower-case letters indicate mass center coordinates and inertial center angle $(x, y, \theta_x, \theta_y)$. The following identities are utilized here in order to describe the relations between geometric centers and inertial centers of each mass element,

$$\begin{array}{lll} x_i = X_i + \xi_i\cos\Omega t - \zeta_i\sin\Omega t & , & \theta_{xi} = \Theta_{xi} + \mu_i\cos\Omega t - \eta_i\sin\Omega t \\ y_i = Y_i + \xi_i\sin\Omega t + \zeta_i\cos\Omega t & , & \theta_{yi} = \Theta_{yi} + \mu_i\sin\Omega t + \eta_i\cos\Omega t \end{array} \tag{2}$$

where ξ_i, ζ_i are eccentricity components of static mass imbalance and μ_i, η_i are inclination components of dynamic mass imbalance, relative to a fixed reference frame of each mass element i. Substituting Eq. (2) into (1) gives,

$$\begin{array}{lll} x_c = X_c + \bar{\xi}\cos\Omega t - \bar{\zeta}\sin\Omega t & , & \theta_{xc} = \Theta_{xc} + \bar{\mu}\cos\Omega t - \bar{\eta}\sin\Omega t \\ y_c = Y_c + \bar{\xi}\sin\Omega t + \bar{\zeta}\cos\Omega t & , & \theta_{yc} = \Theta_{yc} + \bar{\mu}\sin\Omega t + \bar{\eta}\cos\Omega t \end{array} \tag{3}$$

where $\bar{\xi}, \bar{\zeta}, \bar{\mu}, \bar{\eta}$ are eccentricity and inclination components of the complete rotor system and are given by,

$$\begin{array}{ll} X_c = \Sigma_i\left(m_i X_i\right)/M_{tot} & \bar{\xi} = \Sigma_i\left(m_i\xi_i\right)/M_{tot} \\ Y_c = \Sigma_i\left(m_i Y_i\right)/M_{tot} & \bar{\zeta} = \Sigma_i\left(m_i\zeta_i\right)/M_{tot} \\ \Theta_{xc} = \Sigma_i\left(\left(I_{ti}-I_{pi}\right)\Theta_{xi} - m_i Y_i z_i\right)/I_{tot} & \bar{\mu} = \Sigma_i\left(\left(I_{ti}-I_{pi}\right)\mu_i - m_i\zeta_i z_i\right)/I_{tot} \\ \Theta_{yc} = \Sigma_i\left(\left(I_{ti}-I_{pi}\right)\Theta_{yi} + m_i X_i z_i\right)/I_{tot} & \bar{\eta} = \Sigma_i\left(\left(I_{ti}-I_{pi}\right)\eta_i + m_i\xi_i z_i\right)/I_{tot} \end{array} \tag{4}$$

It is easy to recognize the similarity between Eq. (1) and (3). In both cases, the transformation from inertial centers to geometric centers and vice-versa requires identical rotation transformation of different eccentricity and inclination components. Hence. the inertial centers of the complete rotor can be observed as an independent set of coordinates with

static and dynamic imbalance. This may be interpreted incorrectly with a conclusion that knowledge of these parameters is sufficient for implementation of inertial centering control algorithms. In fact, it will be shown here that in the presence of gyroscopic effects, more information is needed for inertial centering.

2.2. Controller Derivation

Let $\mathbf{q}_c \in \mathbb{R}^n$ and $\mathbf{q}_g \in \mathbb{R}^n$ be vectors of generalized coordinates of the inertial centers and geometric centers of each rotor element, respectively. Then it is possible to define a periodic matrix $Q_{cg}(t) \in \mathbb{R}^{n\times r}$ and a vector $\mathbf{u}_{ub} \in \mathbb{R}^r$ of the imbalance magnitudes such that,

$$\mathbf{q}_c = \mathbf{q}_g + Q_{cg}(t)\,\mathbf{u}_{ub} \tag{5}$$

Note that $Q_{cg}(t)$ is block diagonal of 2D rotation matrices, $R(\Omega t)$. This can be recognized from the relations between geometric centers and inertial centers of each mass element in Eq. (2), which can be formulated by (5) with the following definitions, $\mathbf{q}_c \triangleq \begin{bmatrix} x & y & \theta_x & \theta_y \end{bmatrix}^T$, $\mathbf{q}_g \triangleq \begin{bmatrix} X & Y & \Theta_x & \Theta_y \end{bmatrix}^T$, $\mathbf{u}_{ub} \triangleq \begin{bmatrix} \xi & \zeta & \mu & \eta \end{bmatrix}^T$ and $Q_{cg}(\Omega t) \triangleq \mathrm{diag}\begin{pmatrix} R(\Omega t), & R(\Omega t) \end{pmatrix}$ where,

$$R(\Omega t) = \begin{bmatrix} \cos\Omega t & -\sin\Omega t \\ \sin\Omega t & \cos\Omega t \end{bmatrix} \tag{6}$$

In a flexible rotor system, mass accelerations and gyroscopic forces are taken with respect to the coordinates of inertial centers while damping and elastic stiffness forces are taken with respect to the coordinates of geometric centers. Hence, the general set of differential eqnarrays of motion (EoM) for a discrete model of a free-free balanced rotor is given in the following general matrix form,

$$M\ddot{\mathbf{q}}_c + \Omega G\dot{\mathbf{q}}_c + D\dot{\mathbf{q}}_g + K\mathbf{q}_g = \mathbf{f}_{ex}(t) \tag{7}$$

where $M \in \mathbb{R}^{n\times n}$ is a diagonal and positive definite mass matrix, $D \in \mathbb{R}^{n\times n}$ is a symmetric matrix representing external damping, $G \in \mathbb{R}^{n\times n}$ is skew-symmetric and represents gyroscopic forces, $K \in \mathbb{R}^{n\times n}$ is symmetric, positive semi-definite stiffness matrix, $\mathbf{f}_{ex}(t) \in \mathbb{R}^n$ is a vector of external forces and $\Omega \in \mathbb{R}$ is the *nominal* spinning speed of the rotor, while n is the number of system DoFs.

By substituting the imbalance relations from (5), the EoM (7) can be represented in one of the following general forms,

$$M\ddot{\mathbf{q}}_g + (D + \Omega G)\dot{\mathbf{q}}_g + K\mathbf{q}_g = \mathbf{f}_{ex}(t) + \underbrace{\left(M\Omega^2 Q_{cg}(t) - \Omega G\dot{Q}_{cg}(t)\right)}_{\triangleq Q_g}\mathbf{u}_{ub} \tag{8}$$

$$M\ddot{\mathbf{q}}_c + (D + \Omega G)\dot{\mathbf{q}}_c + K\mathbf{q}_c = \mathbf{f}_{ex}(t) + \underbrace{\left(D\dot{Q}_{cg}(t) + KQ_{cg}(t)\right)}_{\triangleq Q_c}\mathbf{u}_{ub} \tag{9}$$

where $Q_g \in \mathbb{R}^{n\times r}$ and $Q_c \in \mathbb{R}^{n\times r}$ are defined as imbalance matrices with respect to generalized geometric and mass center coordinates respectively. Note that internal damping is not included in these eqnarrays. The effect of internal damping will be explained in an extended paper.

Based on the definition of inertial center from (1), it is possible to define a linear transformation from the vector of the generalized coordinates of the mass and inertial centers, $\mathbf{q}_c \in \mathbb{R}^n$, to the vector of the inertial center of the complete rotor, $\mathbf{q}_c \triangleq \begin{bmatrix} x_{ic} & y_{ic} & \theta_{xic} & \theta_{yic} \end{bmatrix}^T$, as follows,

$$M_{ic}\mathbf{q}_{ic} = T_{ic}M\mathbf{q}_c \tag{10}$$

where $M_{ic} = \mathrm{diag}(M_{tot}, M_{tot}, I_{tot}, I_{tot})$, M is the usual stiffness matrix and T_{ic} defines the transformation according to (1).

The goal of the control scheme is to find a control law that leads to,

$$\ddot{\mathbf{q}}_{ic} = -K_{cp}\mathbf{q}_{ic} - K_{cv}\dot{\mathbf{q}}_{ic} \tag{11}$$

where $K_{cp} = \mathrm{diag}\left(k_{ep}, k_{ep}, k_{\tau p}, k_{\tau p}\right)$, $K_{cv} = \mathrm{diag}(k_{ev}, k_{ev}, k_{\tau v}, k_{\tau v})$ and $k_{ev}, k_{ep}, k_{\tau v}, k_{\tau p}$ are positive control gains. Clearly, this type of motion stabilizes the mass center and principal axis of the flexible rotor at the origin, asymptotically.

Substituting (10) to (11) gives,

$$\ddot{\mathbf{q}}_{ic} = M_{ic}^{-1} T_{ic} M \ddot{\mathbf{q}}_c = -K_{cp} M_{ic}^{-1} T_{ic} M \mathbf{q}_c - K_{cv} M_{ic}^{-1} T_{ic} M \dot{\mathbf{q}}_c \tag{12}$$

Since M_{ic}, K_{cp} and K_{cv} are diagonal, multiplying the latter by M_{ic} from the left leads to,

$$T_{ic} M \ddot{\mathbf{q}}_c = -K_{cp} T_{ic} M \mathbf{q}_c - K_{cv} T_{ic} M \dot{\mathbf{q}}_c \tag{13}$$

Substituting $\mathbf{q}_c$, $\dot{\mathbf{q}}_c$, $\ddot{\mathbf{q}}_c$ with $\mathbf{q}_g$, $\dot{\mathbf{q}}_g$, $\ddot{\mathbf{q}}_g$ gives,

$$T_{ic} M \ddot{\mathbf{q}}_g = -K_{cp} T_{ic} M \mathbf{q}_g - K_{cv} T_{ic} M \dot{\mathbf{q}}_g + \left(\left(\Omega^2 I - K_{cp} \right) T_{ic} M Q_{cg}(t) - K_{cv} T_{ic} M \dot{Q}_{cg}(t) \right) \mathbf{u}_{ub} \tag{14}$$

Then, substituting $M\ddot{\mathbf{q}}_g$ from (8) to the latter, results in the following control law,

$$\begin{aligned} T_{ic} \mathbf{f}_{\mathrm{ex}}(t) = & \left(T_{ic} K - K_{cp} T_{ic} M \right) \mathbf{q}_g \\ & + \left(T_{ic} (D + \Omega G) - K_{cv} T_{ic} M \right) \dot{\mathbf{q}}_g \\ & + \left(-K_{cp} T_{ic} M Q_{cg}(t) + \left(T_{ic} \Omega G - K_{cv} T_{ic} M \dot{Q}_{cg} \right)(t) \right) \mathbf{u}_{ub} \end{aligned} \tag{15}$$

In the case of linearized AMB forces, $\mathbf{f}_{ex}$ takes the following form:

$$\mathbf{f}_{ex} = -K_h \mathbf{q}_g - B_{ex} K_i \mathbf{i} \tag{16}$$

where $K_h \in \mathbb{R}^{n \times n}$ is a square-diagonal matrix with negative AMB stiffness constants, $K_i \in \mathbb{R}^{q \times q}$ is a square-diagonal matrix with AMB current constants, $B_{ex} \in \mathbb{R}^{n \times q}$ is the input matrix of AMB forces and q is the number of AMBs control currents. Substituting the latter in Eq. 15 leads to,

$$\mathbf{i} = \underbrace{K_{\mathrm{fb1}}}_{q \times n} \mathbf{q}_g + \underbrace{K_{\mathrm{fb2}}}_{q \times n} \dot{\mathbf{q}}_g + \underbrace{K_{\mathrm{ff}}(\Omega t)}_{q \times r} \mathbf{u}_{ub} \tag{17}$$

where $K_{\mathrm{fb1,2}} \in \mathbb{R}^{q \times n}$ are feedback gain matrices and $K_{\mathrm{ff}}(\Omega t)$ is a periodic time dependent feedforward gain matrix, given by,

$$\begin{aligned} K_{\mathrm{fb1}} &= (T_{ic} B_{ex} K_i)^{-1} \left(K_{cp} T_{ic} M - T_{ic} (K + K_h) \right) \\ K_{\mathrm{fb2}} &= (T_{ic} B_{ex} K_i)^{-1} \left(K_{cv} T_{ic} M - T_{ic} (D + \Omega G) \right) \\ K_{\mathrm{ff}}(\Omega t) &= (T_{ic} B_{ex} K_i)^{-1} \left(K_{cp} T_{ic} M Q_{cg}(\Omega t) + (K_{cv} T_{ic} M - T_{ic} \Omega G) \dot{Q}_{cg}(\Omega t) \right) \end{aligned} \tag{18}$$

The feedback gain matrices act on the geometric centers and their time derivatives, which are assumed to be measured (in a state-feedback configuration). On the other hand, the feedforward controller requires the imbalance coefficients of each rotor element $(\xi_i, \zeta_i, \mu_i, \eta_i)$ which are assumed to be constant and are, in general, unknown. By considering the typical structure of T_{ic}, M, G, $Q_{cg}(\Omega t)$ and $\dot{Q}_{cg}(\Omega t)$, it is easy to show that the feedforward controller is also given by,

$$K_{\mathrm{ff}}(\Omega t) \mathbf{u}_{ub} = (T_{ic} B_{ex} K_i)^{-1} \left(K_{cp} Q(\Omega t) M_{ic} \bar{\mathbf{u}}_{ub} + K_{cv} \dot{Q}(\Omega t) M_{ic} \bar{\mathbf{u}}_{ub} - \Omega^2 Q(\Omega t) \boldsymbol{\psi}_{ub} \right) \tag{19}$$

where $Q(\Omega t) = \mathrm{diag}\left(R(\Omega t), R(\Omega t) \right)$ is block diagonal of 2D rotation matrices, $\bar{\mathbf{u}}_{ub} \triangleq \begin{bmatrix} \bar{\xi} & \bar{\zeta} & \bar{\mu} & \bar{\eta} \end{bmatrix}^T$ is a vector of the imbalance parameters of the complete rotor and $\boldsymbol{\psi}_{ub} = \begin{bmatrix} 0 & 0 & \psi_\mu & \psi_\eta \end{bmatrix}^T$ is a gyroscopic imbalance coefficients vector where $\psi_\mu = \Sigma \frac{I_{pi}}{I_{ti}} \left(I_{ti} - I_{pi} \right) \mu_i$ and $\psi_\eta = \Sigma \frac{I_{pi}}{I_{ti}} \left(I_{ti} - I_{pi} \right) \eta_i$. As expected, the feedforward control law requires the imbalance coefficients $\bar{\xi}, \bar{\zeta}, \bar{\mu}, \bar{\eta}$ which express the mechanical imbalance of the complete rotor system as in Eq. (3). However, additional two imbalance coefficients are needed for the imbalance compensation: ψ_μ and ψ_η. These coefficients are aimed at compensating the gyroscopic moments and hence, are referred to here as, gyroscopic imbalance coefficients.

3. Damping and Stability Analysis

From 11, the control law stabilizes the inertial center of the complete rotor system at the geometric origin of the system support. However, zero radial forces and gyroscopic moments are achieved only if the assumption of rigid-like rotor is valid. This means that the rotor elements must not carry any relative movement with respect to each other. Essentially, relative motion of the rotor elements is a result of rotor deformation vibrations and thus, inertial centering is fully achieved only if the rotor is not vibrating.

A flexible system response, due to an abrupt excitation is a collection of periodic trajectories. In the context of rotor systems, the response is a collection of periodic orbits with natural frequencies, and the frequency of the input excitation.

The orbits with natural frequencies include bending vibrations due to stored elastic energy in the flexible rotor. This energy must be dissipated during the transient response and this may be achieved in the presence of internal or external damping forces. In the absence of a meaningful damping, intense enough to allow a short transient response, artificial external damping can be applied in the control scheme.

Roughly speaking, from control theory point of view, if the energy of the system is completely dissipated around the equilibrium, this means that the equilibrium is exponentially stable. It will be demonstrated here, that asymptotic stability can be achieved by adding an external time-varying damping element to the inertial centering control law, as follows,

$$\mathbf{i} = \underbrace{K_{\text{fb1}}\mathbf{q}_g + K_{\text{fb2}}\dot{\mathbf{q}}_g + K_{\text{ff}}(\Omega t)\,\mathbf{u}_{ub}}_{\text{Inertial centering}} + \underbrace{k_d(t)\,K_i^{-1}D\dot{\mathbf{q}}_g}_{\text{Artificial damping}} \tag{20}$$

where $k_d(t)$ is a *time-depended damping coefficient* which is designed manually to dissipate stored energy of bending vibrations. In (20), K_i is the AMB current gain matrix from (16) and D is the rotor damping matrix from (8) and (9). The choice of this particular external damping mechanism is simply based on the natural damping physics of the rotor, without the destabilizing circulatory forces, which may be caused by internal damping.

A state representation of the flexible rotor system 8 may be given by defining a state vector $\mathbf{x}^T = \begin{bmatrix} \mathbf{q}_g & \dot{\mathbf{q}}_g \end{bmatrix}^T$ as follows,

$$\frac{d\mathbf{x}}{dt} = \begin{bmatrix} 0_{n\times n} & I_{n\times n} \\ -M^{-1}(K+K_h) & -M^{-1}(D+\Omega G) \end{bmatrix}\mathbf{x} + \begin{bmatrix} 0_{n\times r} \\ M^{-1}Q_g(t) \end{bmatrix}\mathbf{u}_{ub} + \begin{bmatrix} 0_{n\times q} \\ -M^{-1}B_{ex}K_i \end{bmatrix}\mathbf{i} \tag{21}$$

Then, substituting the control currents from (17), results with the state space representation of the closed loop rotor system. This would lead to the following general structure,

$$\dot{\mathbf{x}} = \widetilde{A}\mathbf{x} + \widetilde{B}(t)\,\mathbf{u}_{ub} \tag{22}$$

where $\widetilde{A} \in \mathbb{R}^{n\times n}$ is a constant square matrix and $\widetilde{B}(t) \in \mathbb{R}^{n\times r}$ is a periodic input matrix.

Some general stability considerations are now explained. As seen in (11), the inertial center closed loop system is exponentially stable. However, this does not imply that the closed loop rotor system given by (22) is also stable. As a matter of fact, it will be shown in following sections that there are geometric and mechanical conditions for the rotor in order to assure stability. As for the stable regions, where the eigenvalues of $\widetilde{A}$ from (22) are all in the OLHP, it is well known that if the system is exponentially stable, it is also BIBO stable. Then, since the input excitation $\widetilde{B}(t)\,\mathbf{u}_{ub}$ is bounded, the state response is also bounded. So, as long as the air gap of the AMBs is large enough to allow the rotor to orbit inside without contact, the system is stable.

4. Case Study and Numerical Results

An 8-DoF flexible rotor model supported by two AMBs is utilized for the numerical results which are presented in the following figures. In this model, three concentrated masses (m_1, m_2, m_3) are lumped by massless shaft-connections with identical elastic characteristics. The dynamic bending of the shaft is in two mutually perpendicular lateral directions (x and y) and the central mass (m_2) has transverse and polar moments of inertia (I_t, I_p), meaning that it can rotate in x and y directions (θ_x, θ_y) and excite gyroscopic effects. The AMBs are located at the end masses (m_1, m_3) and are modeled as linearized AMBs with a negative stiffness. Fig. 1 shows an illustration of the AMB-rotor system (right) and a block diagram of the control scheme (left). The artificial damping and inertial centering blocks in the diagram, implement (20). The EoM of the 8-DoF AMB-rotor system are given as follows,

$$\begin{aligned}
m_1\ddot{x}_1 &= -k_1\left(x_1 - x_2 + \theta_y L_1\right) + m_1\Omega^2\left(\xi_1\cos(\Omega t) - \zeta_1\sin(\Omega t)\right) + F_{AMB,x1} \\
m_1\ddot{y}_1 &= -k_1\left(y_1 - y_2 - \theta_x L_1\right) + m_1\Omega^2\left(\xi_1\sin(\Omega t) + \zeta_1\cos(\Omega t)\right) + F_{AMB,y1} \\
m_2\ddot{x}_2 &= -k_1\left(x_2 - x_1 - \theta_y L_1\right) - k_2\left(x_2 - x_3 + \theta_y L_2\right) + m_2\Omega^2\left(\xi_2\cos(\Omega t) - \zeta_2\sin(\Omega t)\right) \\
m_2\ddot{y}_2 &= -k_1\left(y_2 - y_1 + \theta_x L_1\right) - k_2\left(y_2 - y_3 - \theta_x L_2\right) + m_2\Omega^2\left(\xi_2\sin(\Omega t) + \zeta_2\cos(\Omega t)\right) \\
I_t\ddot{\theta}_x &= -k_1 L_1\left(\theta_x L_1 + y_2 - y_1\right) - k_2 L_2\left(\theta_x L_2 + y_3 - y_2\right) - I_p\Omega\dot{\theta}_y + \left(I_t - I_p\right)\Omega^2\left(\mu\cos(\Omega t) - \eta\sin(\Omega t)\right) \\
I_t\ddot{\theta}_y &= -k_1 L_1\left(\theta_y L_1 + x_1 - x_2\right) - k_2 L_2\left(\theta_y L_2 + x_2 - x_3\right) + I_p\Omega\dot{\theta}_x + \left(I_t - I_p\right)\Omega^2\left(\mu\sin(\Omega t) + \eta\cos(\Omega t)\right) \\
m_3\ddot{x}_3 &= -k_2\left(x_3 - x_2 - \theta_y L_2\right) + m_3\Omega^2\left(\xi_3\cos(\Omega t) - \zeta_3\sin(\Omega t)\right) + F_{AMB,x3} \\
m_3\ddot{y}_3 &= -k_2\left(y_3 - y_2 + \theta_x L_2\right) + m_3\Omega^2\left(\xi_3\sin(\Omega t) + \zeta_3\cos\zeta(\Omega t)\right) + F_{AMB,y3}
\end{aligned} \tag{23}$$

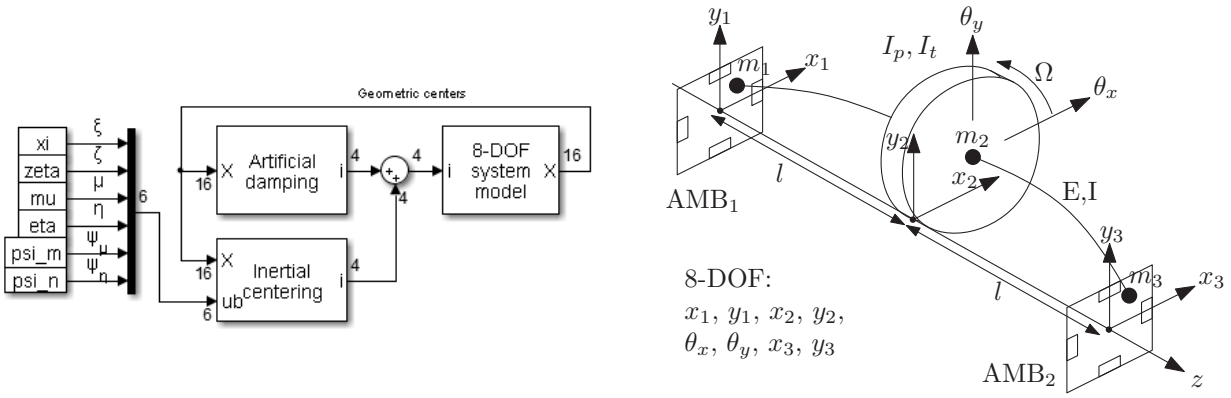

Fig. 1 8-DOF model of a flexible rotor-AMB system (left) and a block diagram of the control scheme (right)

The model parameters were chosen such that the rotor is transversely symmetric, meaning that $m_1 = m_3 \triangleq m$ and $k_1 = k_2 \triangleq k_s$. In this relatively simple case, it can be shown that without any damping mechanism, the controller can bring the rotor to a marginal stability. The development of the conditions for marginal stability is based on analytic investigation of closed loop pole location, and only the result is given here,

$$\begin{aligned} &\text{I.} \quad k_{ep}, k_{ev}, k_{\tau p}, k_{\tau v} > 0 \\ &\text{II.} \quad 4I_t k_s \left(I_t - I_p + 2L^2 m\right) + I_p^2 m\Omega^2 > 0 \\ &\text{III.} \quad 2L^2 m \neq I_p - I_t \end{aligned} \tag{24}$$

The complete derivation of these conditions will be presented in an extended paper. Note that if these conditions do not hold, the closed loop rotor system is unstable, despite the stability of the closed loop inertial center system. The values of model parameters for the simulation where chosen such that the stability conditions are satisfied. As mentioned above, exponential stability may be achieved by adding an external damping module to the control scheme. The location of the poles as a function of k_d, which indicate on the damping intensity, is presented in figure 2. It can be seen that the poles location start at the imaginary axis and move to the OLHP as the intensity of the damping increases.

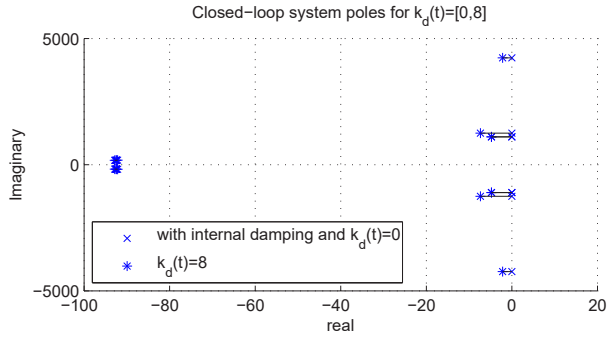

Fig. 2 Pole location map of the closed loop system as a function of k_d, the damping intensity. The system is marginally stable for $k_d = 0$ and the poles move to the OLHP as it increases.

The critical speed of the first bending mode is at 10.55krpm and the rotor is spinning at 15krpm. The imbalance coefficient values are given in Table. 1, along with the corresponding force and moment amplitudes which are calculated by $m\Omega^2\sqrt{\xi^2+\zeta^2}$ and $\left|I_t - I_p\right|\Omega^2\sqrt{\mu^2+\eta^2}$, respectively. Each mass carries different imbalance amplitude and phase, resulting in more than 420N synchronous forces and 8.4Nm synchronous moments.

Table 1 Imbalance amplitudes. Each mass carries different imbalance amplitude and phase.

mass	Imbalance values	Force\moment amplitude
$m_1 = 0.8334\,[\text{kg}]$	$\xi_1 = 26.4\,[\mu\text{m}]$, $\zeta_1 = 45.7\,[\mu\text{m}]$	108.6[N]
$m_2 = 11.322\,[\text{kg}]$	$\xi_2 = 3.5\,[\mu\text{m}]$, $\zeta_2 = 172[\mu\text{m}]$	420.4[N]
$\lvert I_t - I_p\rvert = 0.023\,[\text{kg m}^2]$	$\mu_2 = 119\,[\mu\text{rad}]$, $\eta_2 = 89.2\,[\mu\text{rad}]$	8.383[Nm]
$m_3 = 0.8334\,[\text{kg}]$	$\xi_3 = 0$, $\zeta_3 = 26.4\,[\mu\text{m}]$	54.3[N]

The time response of the displacements at the AMB planes is presented in Fig. 3 and the AMB forces and artificial damping intensity are presented in Fig. 4. The simulation starts with an abrupt imbalance excitation and during the first 0.3s time slot, the artificial damping intensity is zero. During this time (bottom of Fig. 3), the inertial centers are regulated, but the elastic energy of the rotor is not dissipated and the rotor is vibrating, as illustrated in Fig. 5 (left). Since the rotor is vibrating, the AMBs still apply a relatively large value of force, although the inertial centers have converged to zero. After 0.3s the artificial damping is set to a maximum level, and then, it is decreased monotonically back to zero after 4.5s. At this point, the stored elastic energy is fully dissipated, the rotor is inertially-centered and the AMB forces are very close to zero. Fig. 5 (right) shows the orbits of the mass elements of the rotor at this stage.

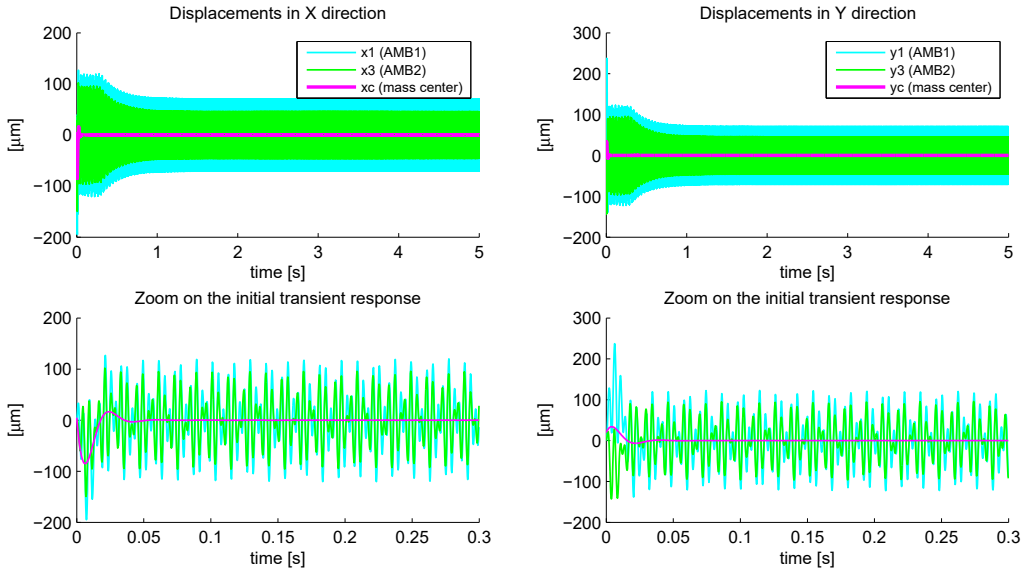

Fig. 3 Displacements of the geometric centers at the AMB planes and the mass center of the complete rotor

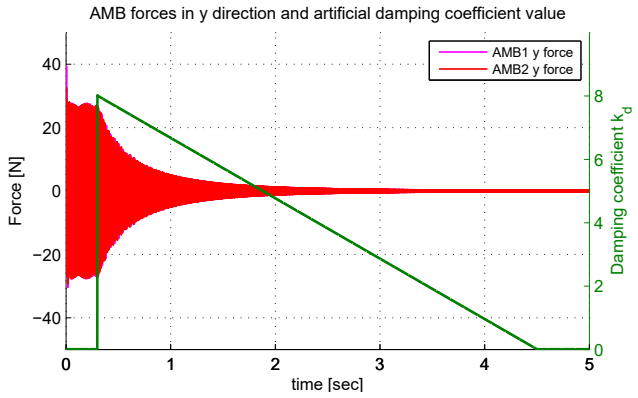

Fig. 4 AMB forces and time varying artificial damping intensity

5. Conclusions

An inertial centering control scheme for a general flexible AMB-rotor systems with multiple mass imbalances was suggested in this paper. It was shown that in the absence of gyroscopic effects, the inertial center of the complete rotor can be observed as an independent set of coordinates with static and dynamic imbalance. However, in the presence of gyroscopic effects, more information is needed to implement an imbalance compensation controller. The stability of the control scheme was discussed and a case study of 8-DoF rotor system was presented, along with a pole location analysis. A numerical example, where each mass element of the rotor is subjected to mass imbalance with different amplitude and phase, was presented. The results showed that a massively imbalanced flexible rotor can be inertially-centered by applying a relatively small control forces, which eventually vanish in the steady state.

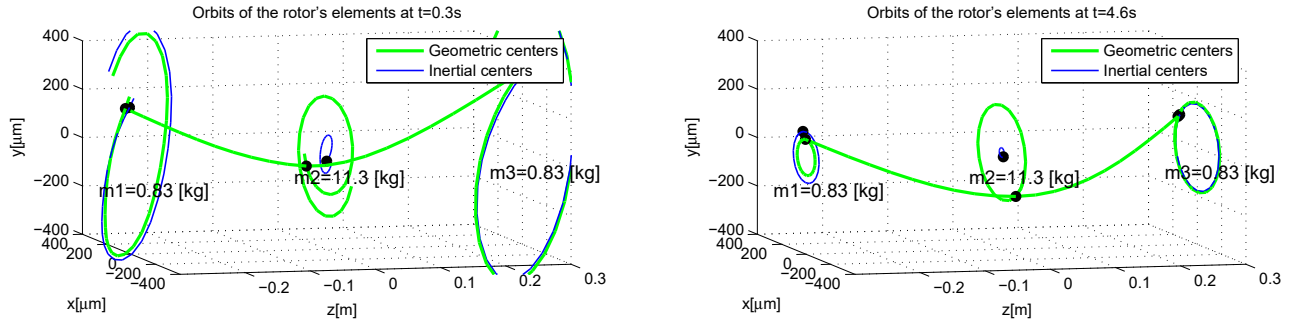

Fig. 5 Orbits of the rotor's elements during the transient response at the beginning of the simulation where the rotor is vibrating (left). and during the steady state response where the rotor is inertially-centered and the AMB forces are zero (right).

References

Becker, F. B., Heindel, S. and Rinderknecht, S., Active Vibration Isolation of a Flexible Rotor Being Subject to Unbalance Excitation and Gyroscopic Effect Using H_∞-Optimal Control. In Proceedings of the 9th IFToMM International Conference on Rotor Dynamics (2015), pp. 1727-1739. Springer International Publishing.

Chen, Q., Liu, G. and Zheng, S., Suppression of imbalance vibration for AMBs controlled driveline system using double-loop structure. Journal of Sound and Vibration, Vol. 337 (2015), pp. 1-13.

Fang, J., Zheng, S. and Han, B., AMB vibration control for structural resonance of double-gimbal control moment gyro with high-speed magnetically suspended rotor. Mechatronics, IEEE/ASME Transactions on, Vol. 18 (2013), No. 1, pp. 32-43.

Levy, R. and Arogeti, S., Inertial centering approach for high speed flexible rotor systems supported by AMBs, 13th International Conference on Control Automation Robotics & Vision (2014), pp. 289-294.

Lum, K. Y., Coppola, V. T. and Bernstein, D. S., Adaptive virtual autobalancing for a rigid rotor with unknown mass imbalance supported by magnetic bearings. Journal of vibration and acoustics, Vol. 120, No. 2 (1998), pp. 557-570.

Lum, K. Y., Coppola, V. T. and Bernstein, D. S., Adaptive autocentering control for an active magnetic bearing supporting a rotor with unknown mass imbalance. IEEE Transactions on Control Systems Technology, Vol. 4, No. 5 (1996), pp. 587-597.

Riemann, B., Sehr, M. A., Schittenhelm, R. S. and Rinderknecht, S., Robust control of flexible high-speed rotors via mixed uncertainties. In IEEE European Control Conference (ECC, 2013), pp. 2343-2350.

Sahinkaya, M. N., Abulrub, A. H. G. and Burrows, C. R., An adaptive multi-objective controller for flexible rotor and magnetic bearing systems. Journal of Dynamic Systems, Measurement, and Control, Vol.133 (2011), No.3, pp. 031003.

Schittenhelm, R. S., Riemann, B. and Rinderknecht, S., Modal H_∞-control in the context of a rotor being subject to unbalance excitation and gyroscopic effect. In ASME Turbo Expo 2013: Turbine Technical Conference and Exposition.

Tang, E., Fang, J., Zheng, S. and Jiang, D., Active Vibration Control of the Flexible Rotor to Pass the First Bending Critical Speed in High Energy Density Magnetically Suspended Motor. Journal of Engineering for Gas Turbines and Power, Vol. 137 (2015a), No. 11, pp. 112501.

Tang, E., Fang, J. and Han, B., Active Vibration Control of the Flexible Rotor in High Energy Density Magnetically Suspended Motor With Mode Separation Method. Journal of Engineering for Gas Turbines and Power, Vol. 137 (2015b), No. 8, pp. 082503.

Tang, E., Han, B. and Zhang, Y., Optimum Compensator Design for the Flexible Rotor in Magnetically Suspended Motor to Pass the First Bending Critical Speed. IEEE Transactions on Industrial Electronics, Vol. 63 (2016), No. 1, pp. 343-354.

Xiang, M. and Wei, T., Autobalancing of high-speed rotors suspended by magnetic bearings using LMS adaptive feedforward compensation. Journal of Vibration and Control, Vol. 20, No. 9 (2014), pp. 1428-1436

Yuan Ren, Dan Su, and Jiancheng Fang., Whirling modes stability criterion for a magnetically suspended flywheel rotor with significant gyroscopic effects and bending modes. IEEE Transactions on Power Electronics, Vol.28 (2013), No.12, pp. 58905901.